NASA CR-151946

MODELING STUDIES FOR A MARS PENETRATOR HEAT FLOW MEASUREMENT

Stephen J. Keihm and Marcus G. Langseth
Lamont-Doherty Geological Observatory of Columbia University
Palisades, New York, 10964

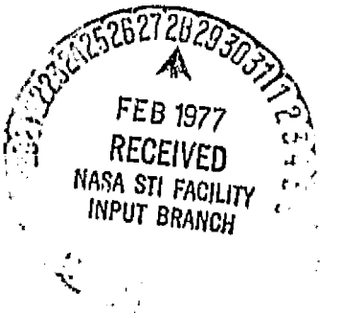

Technical Report No. CU-1-77

At present, two different design concepts are being considered for the purpose of measuring heat flow as part of a Mars penetrator mission. The first of the tentative designs utilizes temperature sensors emplaced along the trailing umbilicus at regularly spaced intervals, no greater than 1m, which will be thermally coupled to the adjacent regolith radiatively and possibly convectively (open hole configuration) or conductively (collapsed hole configuration). Depending upon the depth of penetration, some or all of the umbilicus sensors will be subject to thermal perturbations due to diurnal and seasonal temperature variations, dissipation of initial heat and heat deposited during emplacement, and transients from energy released by the 10 or 20 watt RTG contained within the penetrator body.

The second of the heat flow designs considered requires the radial deployment of two or more low thermal mass temperature sensors outward from the penetrator body over a vertical (depth) range on the order of 1m. Transient effects will include the dissipation of initial heat of the sensor and accompanying radial deployment arm and the eventually dominant thermal pulse originating from the penetrator initial heat and RTG power supply. Seasonal soil temperature variations may also be important if penetration depths do not exceed 5 m.

N77-17395

(NASA-CR-151946) MODELING STUDIES FOR A MARS PENETRATOR HEAT FLOW MEASUREMENT (Lamont-Doherty Geological Observatory) 29 p HC A03/MF A01 CSCL 20D

Unclas G3/34 14990

It is the purpose of this report to describe results of numerical simulations used to investigate the feasibility and relative merits of each of the proposed design concepts for a Mars penetrator heat flow measurement. It is to be noted that all discussion is of a theoretical and interpretational nature. A complimentary investigation of the engineering and design problems associated with each of the proposed heat flow measurement modes will be essential and perhaps overriding in any final choice of experiment design.

I. Umbilicus Sensors

The effects of annual variations and RTG-induced thermal transients upon umbilicus temperatures in the open hole configuration have been previously investigated (FY 1976 Progress Report on a Feasibility Study Evaluating the Use of Surface Penetrators for Planetary Exploration, NASA TM X-73, 181). Results of numerical models incorporating radiative and conductive thermal linkages indicated that the large annual subsurface temperature variations expected on Mars should be well coupled with the umbilicus sensors and could be accounted for given a sufficient time window of data (at least 0.5 martian years). Significant RTG transient effects, propagated radiatively, will dominate umbilicus temperature histories within 1-2 m of the penetrator tail before one half martian year has elapsed. Thus, if annual variations are important at these depths, reliable mean temperature estimates will not be feasible. At depths where annual variations are negligible ($\gtrsim$ 5-8 m), the necessary time frame of umbilicus data free of penetrator transient effects would be reduced to the equilibration time of initial heat deposition (on the order of tens of days). In such a case, meaningful mean temperature estimates could feasibly be made as near as 1m from the penetrator tail.

The object of the present study of umbilicus models was to assess the near surface effects of diurnal and annual temperature variations. Two specific effects were investigated: (1) The effect of a temperature dependent regolith thermal conductivity on the mean temperature profile; and, (2) The effect of diurnal variations propagating radiatively down an open hole.

- Temperature Dependent Thermal Conductivity -

At the Apollo 15 and 17 lunar heat-flow sites, 35-45°K mean temperature differences were observed between the surface and depths greater than 10 cm. The interior heat flux can contribute only a negligible proportion of such gradients. The phenomenon can only be explained by the rectifying effect of a strongly temperature dependent thermal conductivity in the upper few centimeters. During the warm lunar day, heat is transferred more effectively into the lunar surface than it can be removed during the cold lunar night. To conserve net flux over a lunation, a mean temperature gradient is established, confined mainly to the upper few centimeters. At the Apollo sites, variations of near surface thermal conductivity by factors of 2.5-3.5 were required to produce the observed mean temperature gradient. For the Mars situation, thermal conductivity temperature variation is expected to be limited by the dominance of the interstitial gas in the heat transfer process. Laboratory measurements, under simulated lunar and martian conditions (Fountain, J.A. and West, E.A., 1970, J.G.R. 75, 4063-4069), resulted in a doubling of thermal conductivity under vacuum conditions between 190 and 300°K, but only a 30% increase over the same range in the presence of CO_2 at 7 mb. As an upper limit to the temperature dependence effect, we have assumed that the Mars regolith thermal conductivity increases ~ 80% between 160 and 290°K, a feasible surface temperature

variation at near equatorial latitudes. This corresponds to a variation of $\sim$ 25% between 170 and 230°K, a feasible range of seasonal temperature variation in the upper meter.

Mean temperature effects due to the diurnal heating cycle were calculated for two different levels of conductivity. Results are shown in Figure 1. As expected, over the short Mars diurnal period, (relative to the moon), the magnitude of the mean temperature change is small (3.5-6.5°K) and limited to depths less than 10 cm. Even if a conductivity level as high as 0.001 w/cm°K characterized the upper layers, it is clear that martian diurnal mean temperature effects need not be considered as a perturbing factor on steady-state gradient measurements made below 20 cm.

The much longer period annual variations on Mars, although of smaller amplitude, will penetrate to meter depths, and could result in significant mean temperature gradients as deep as two meters. The results shown in Figure 2 assume a seasonal surface temperature variation of $T_s = 200 + 30 \sin(\omega t)$ where ω is the orbital frequency. Note that although the total effect is less than 1°K, it extends over a depth range of $\sim$ 2m, and is comparable to feasible steady-state gradients which could be produced by internal heat loss. Although the degree of conductivity temperature dependence employed in the models is most likely too high, the models do show that mean temperature gradients measured at depths shallower than two meters will require cautious interpretation. If umbilicus sensors were closely spaced ($\sim$ 0.5 m), the degree of linearity of the mean temperature profile could provide one possible check on the reliability of interpreting a shallow mean temperature gradient in terms of internal heat loss.

- Open Hole Radiative Propagation of Diurnal Variations -

Detailed modeling of the lunar heat flow probe-borestem geometry

showed that radiative transfer of high frequency diurnal variations resulted in enhanced propagation (relative to the adjacent regolith) of the diurnal wave along the open hole. The degree of amplification was proportional to the insulating properties of the surrounding regolith, i.e. larger and deeper diurnal variations were produced for lower conductivity surroundings. In addition, small mean temperature differences were maintained between the borestem and adjacent regolith to depths of 60 cm due to the lower lunation mean temperature of the hole "cap", i.e. the section of borestem which protruded above the lunar surface.

Similar effects can be anticipated for a Mars penetrator open hole deployment with the afterbody analogous to the protruding lunar borestem. Figure 3 illustrates the effect for a "worst case" model with a 9 cm diameter hole surrounded by a regolith of the lowest expected Mars thermal conductivity of $k = 2 \times 10^{-4}$ w/cm°K. The afterbody was modeled simply as a solid cylindrical section of perfect conductor capping the open hole with a height 18 cm above the surface and a mass of 2.3 kg. Results indicate that perceptible diurnal effects could be expected along the hole wall to depths of 50 cm, even though diurnal variations in the undisturbed regolith are negligible at a depth of 20 cm. Such an effect must be anticipated if the hole remains open, and even time averaged borehole temperatures may not accurately reflect the regolith gradient at depths shallower than 50 cm.

Radially Deployed Sensors

Assuming sufficient radial extension (9 or more cm from penetrator body) and the limitation of impact-generated shock and deformation effects to within 1-2 cm of the penetrator, the primary factor affecting the measurement of preimpact regolith temperatures will be the thermal linkage from the penetrator body along the radial deployment arm (hereafter referred to as the "probe") to the sensor. The penetrator and radial probe can be

expected to maintain preimpact temperatures on the order of 50-150°K above martian regolith temperatures. Impact generated heat will add to this difference, although most of the generated heat can be expected to reside in the penetrator nose and along a thin soil contact layer within 1mm of the penetrator body. The presence of a 10 or 20 W power source will prevent the penetrater from equilibrating substantially to the regolith temperature. The primary objective of the models to be discussed is the determination of a feasible radial extension design which will allow an accurate measurement of the undisturbed regolith temperature gradient to be made before the penetrator thermal pulse significantly affects the preimpact thermal regime.

Precise modeling of a cylindrical penetrator with one or more radial extension arms requires a three dimensional geometry. However, since the penetrator-induced disturbance to the radial probe equilibration will be transmitted primarily along the extension arm itself, the problem can be converted to two dimensions without significantly altering the early time history of penetrator-radial probe heat exchange. The models presented assume that the penetrator can be represented as an infinite heat reservoir at an elevated temperature T'_o one hundred degrees above the undisturbed regolith. The "infinite reservoir" assumption is justified by the much larger thermal mass of the penetrator body compared to the radial probe. The 100°K temperature difference is assumed to include all preimpact and impact generated heat appropriate to the base of the radial probe. Schematics of the actual geometry and equivalent modeling geometry are shown below.

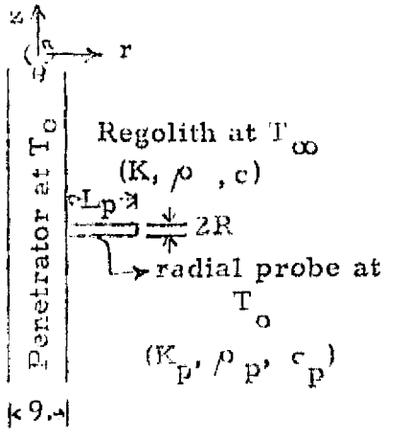

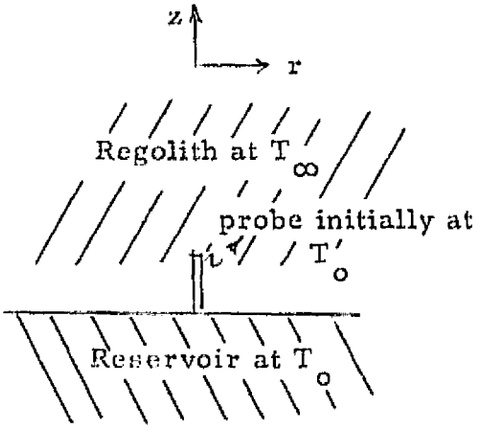

Initial probe temperature is also assumed to be T_o, 100°K above the surrounding regolith. The probe was assumed to be made of stainless steel with thermal conductivity k_p = 0.138 w/cm°K and ρc_p = 3.6 w sec/cm^3°K. The choice of stainless steel is a "worst" case in the sense that the large conductivity will enhance effects from the penetrator reservoir and the large volumetric heat capacity will slow equilibration to the surrounding soil temperature for a given probe diameter. However, the design requirement of a probe material of sufficient strength to allow penetration into highly compacted regolith may necessitate a choice of probe material of comparable thermal properties.

The effects of four parameters were examined in the model runs, radial probe length L_p, probe diameter R, regolith conductivity k, and probe conductivity, k_p. In all models a regolith heat capacity of ρ = 1.0 w sec/cm^3 °K was assumed. Initial probe temperature T_o = 200°K and regolith temperature T_∞ = 100°K were used for convenience. All heat transfer was assumed conductive. Results are shown in Figures 4-12 where probe temperatures are shown at various distances from the penetrator reservoir versus inverse time for three feasible values of regolith conductivity, K = 2, 5 and 10 x 10^{-4} w/cm°K. Each figure is distinguished by the probe dimensions length and radius. The "x" data represent the transient solution for an infinite cylinder of perfect conductor equilibrating with a low conductivity infinite medium, and serve as a guide for determining the onset and magnitude of the penetrator thermal pulse. At long times ($kt/R^2\rho c_p \gg 1$) the theoretical equilibration curves can be represented by:

$$T(t) - T_\infty = (T_o - T_\infty) * \frac{R^2 \rho c_p}{4kt} \quad (R = \text{probe radius})$$

Thus, at sufficiently long times, if penetrator and end effects are negligible, a linear extrapolation of the inverse time plots to $t \to \infty$ should

provide an accurate estimate of T_∞ even if T_o is not precisely known. The results of Figures 4-8 attempt to show what combinations of probe length (L_p), radius (R) and sensor location will allow accurate extrapolation to the regolith equilibrium temperature T_∞, before the effects of the thermal pulse from the penetrator "reservoir" mask the measurement. Figures 9 and 10 show the effect of a nonuniform initial temperature distribution along the radial extension arm. Figures 11 and 12 examine the advantages to be gained if the radial probe could be made of a much less conductive material than stainless steel, such as wound fiberglass. Specific results can best be discussed by addressing the Figures directly:

Figure 4: (L_p = 9.0; R = 0.05)

Note that for a regolith conductivity of 0.0002, even a sensor located at the probe end (8.75) begins to feel the effects of the penetrator pulse before an accurate extrapolation of the equilibration history could be made. The situation improves considerably for larger regolith conductivities, although penetrator effects begin to be felt at approximately the same time ($\sim$ 1000 sec at the probe end). However, the probe end equilibration is sufficiently linear for the high k = 0.001 case that an extrapolation of the 200-1000 sec curve would provide a T_∞ estimate accurate to 0.1°K. Note also, however, that end effects lead to more rapid cooling at the 8.75 cm position than the theoretical case while at 7.0 cm (2m from probe tip) the equilibration curve matches the theoretical cooldown almost exactly before the onset of penetrator effects. This suggests that a sensor location slightly removed from the probe tip may simplify the extrapolation to soil equilibrium even though the reequilibration will be most rapid at the probe tip.

Figure 5: L_p = 9.0 cm; R = 0.15 cm

Note that even for the high regolith conductivity case, the cooldown curves have been significantly disturbed by t = 800 sec. This is not suf-

ficient time for the 0.15 cm radius probe to substantially equilibrate, and extrapolation results, even for the high k case, would be no better than $\pm 1°K$. If two radially deployed sensors separated by 1 m were to accurately measure a steady state gradient, a minimum absolute temperature accuracy of at least 0.1°K would be required. In actuality, it is feasible that the Mars regolith gradient could be of the order of 0.1°K/m, in which case extrapolation errors would be comparable to the quantity we are attempting to measure.

Figure 6: $L_p = 20.0$ cm ; R 0.05 cm

Here would be the ideal design for a radially deployed sensor. It is to be noted, of course, that a radial extension greater than the penetrator diameter (9cm) would severely complicate the engineering design in that the radial arm would have to be coiled or hinged in some manner prior to deployment. However, if such design complications could be overcome, it can be seen that any sensor positioning between 15 and 20 cm along the extension arm would provide equilibration histories essentially undisturbed by the penetrator pulse out to at least 2000 sec, a sufficient time span for 0.1°K accurate T_∞ estimates to be made. Increased accuracy would be possible with extended time data as long as the sensor location remained unaffected by the penetrator pulse. Ideally, only the sensor precision need limit the accuracy of the T_∞ determination.

Figure 7: ($L_p = 20.0$; $R = 0.15$)

Figure 8: ($L_p = 20.0$; $R = 0.50$)

If the necessary rigidity could not be maintained in a 20 cm extension arm of 0.05 cm radius, the effects of increasing the arm cross section will quickly lead to enhanced penetrator effect and the subsequent limitation of obtainable T_∞ accuracy. Increasing the radius to 0.15 cm may still allow a satisfactory T_∞ extrapolation from a sensor located at least 15 cm

from the penetrator. However, considerably more than 2000 sec of equilibration will be required, with the eventual limitation of penetrator pulse effects. This is seen most clearly for the R = 0.5 case (Figure 8) in which no extension arm location has equilibrated to within 10°K of $T_{(\infty)}$. Even at the probe tip, (19.75) the first effects of the penetrator thermal pulse can be seen as the cooldown curve crosses the theoretical case at 2000 sec. It is clear that any feasible radial extension arm design would require a minimum possible probe radius since it can be seen from the long time theoretical expression (p 7) that the relative equilibration rate will scale inversely with the square of the probe radius. Additionally, the conductive linkage to the penetrator along the extension arm will scale directly with the square of the probe radius

Figure 9: $L_p = 20.0$; $R = 0.05$ } Linear temperature distribution

Figure 10; $L_p = 20.0$; $R = 0.15$ } in probe initially

In Figures 9 and 10 we examine the reliability of the T_∞ extrapolation technique when the initial radial extension arm temperature varies with distance from the penetrator. Such a situation could be imagined if frictional effects are important during the radial extension process. The models shown represent an extreme case in which a 50°K initial temperature difference exists between probe tip and probe base. It can be seen that, with a sufficient time range of data, the initial differences will be smoothed and at extension arm locations greater than 12-15 cm a linear extrapolation of the 1/t cooling curves from 2000 sec out will provide comparable accuracy of $T_{(\infty)}$ estimates as were obtained for the initially isothermal probe cases (Figures 6 and 7). It is to be noted, however, that conductivity estimates made from the slopes of the longtime 1/t curves require knowledge of the initial temperature difference accurate to a comparable degree of the desired k precision.

Figure 11: $L_p = 20.0$; $R = 0.05$; $K_p = K_{ss}/10.0 = 0.0138 w/cm°K$

Figure 12: $L_p = 20.0$; $R = 0.15$; $K_p = K_{ss}/10.0 = 0.0138 w/cm°K$

It has been suggested (Final Report and Recommendations of the Ad Hoc Surface Penetrator Science Committee, 1976) that a much less conductive material, such as wound fiberglass, could be utilized for the radial probes. To examine the extension required for such a probe, equilibration curves have been plotted in Figures 11 and 12 for various radial distances from the penetrator assuming a probe conductivity ten times less than that of stainless steel (K_{ss}). In Figure 11, a probe radius of 0.05 cm is assumed, and it can be seen that sufficient, undisturbed equilibration can be achieved over the full range of expected Mars regolith conductivities by sensors located within 7-9 cm of the penetrator. An extrapolation accuracy of $\pm$ 0.01°K could be achieved after one hour. This is to be contrasted with the stainless steel probe case (Figure 6) in which sensor placements $\geq$ 15 cm would be required for the lower range of expected regolith conductivities. The advantages of requiring a sensor extension no greater than the penetrator diameter are obvious from the design viewpoint.

Figure 12 illustrates the low probe conductivity case for a probe radius of 0.15 cm. Again, the delay of penetrator influence can be seen when compared to the comparable stainless steel case of Figure 7. Sensors located at the critical 9 cm position would equilibrate free of penetrator effects for periods greater than one hour, allowing extrapolation accuracy to an estimated $\pm$ 0.1°K, which would be adequate for all but the lowest expected values of Mars steady state regolith gradients.

In summary, the analysis of purely conductive effects indicates that the possibility of measuring the Mars regolith temperature gradient by the radial extension method is constrained primarily by design limitations.

To measure undisturbed regolith temperatures to ± 0.1°K will require the deployment of a radial extension arm with a high length/cross section ratio . If sensor extension is limited to 9 cm (penetrator diameter), a low conductivity probe, such as wound fiberglass, would yield extrapolation accuracy of ± 0.01°K for a 0.05 cm arm radius and ± 0.1 K for a 0.15 cm arm radius. If a more conductive material were used, radial arm extension greater than 9 cm would be required to insure comparable extrapolation accuracy over the full range of expected regolith conductivities. If the necessary design could be implemented, the success of a heat-flow measurement would then depend on the sufficiency of penetrator emplacement depth. If significant annual variations are present at the measurement depth, it will not be possible to distinguish periodic fluxes from the flux from the interior because of the very small time allowance for unperturbed measurement. The situation worsens for the higher feasible regolith conductivity values, as shown in Figure 13. For a given heat flow, the steady state gradient will decrease inversely with the conductivity. For example, if Mars heat flow is comparable to the measured lunar heat flow (2.0 $\mu w/cm^2$) transient gradients comparable to the steady state gradient will persist to depths of 7-9 m if the regolith conductivity is as high as 0.001 w/cm°K. Such conductivity values have been inferred for selected martian regions from Mariner IR results. Even for the most favorable situation, k = 0.0002 w/cm°K, significant annual effects could persist to 4 m. It should be emphasized that even a theoretical correction for annual effects would not be possible without a reliable estimate of the thermal diffusivity profile from the surface to penetrator depth.

Conclusions and Recommendations

The relative merits of the umbilicus and radial extension techniques for the measurement of Mars heat flow may be summarized as follows:

Umbilicus Deployment:

1) Sufficient time for analysis of transient and seasonal effects for sensors at least 1-2 m removed from the penetrator tail. Effects due to diurnal variations within the borehole will likely obscure interpretation of any measurements within 50cm of the surface. If regolith conductivity is sufficiently temperature dependent ($\sim$ 25% variation over a 60°K range), a mean temperature gradient unrelated to interior heat flow could produce significant interpretation ambiguity to depths of 2 m. Such a dependence is not considered likely in view of the interstitial gas presence on Mars.

2) For sufficient penetration ($>$ 5 m) and sensor spacing $\leq$ 1m, three or more mean temperature measurements could provide added confidence in the estimate of regolith gradient. Possible depth variations of thermal properties could be detected, providing an important constraint on any non-linearity present in the gradient measurement.

3) Even in the absence of sufficient penetration to allow a reliable steady state gradient measurement, one or more umbilicus sensors could still provide data constraining regolith thermal properties and the diurnal and seasonal thermal regime.

Radial Extension Deployment:

1) Excellent thermal contact with the regolith material. If sufficient extension of a low conductivity radial probe could be achieved, a highly accurate measurement of regolith temperature, uncomplicated by radiative and convective thermal linkages, could be made. It should be pointed out that numerical models and convective simulation models (T. Canning, NASA Ames) appear to demonstrate that umbilicus sensors, adequately removed from penetrator and surface effects, should be well coupled with the adjacent regolith. However, the conductive coupling of a slender probe within a particulate soil has been repeatedly demonstrated by laboratory measurements, and must be considered superior in this respect.

2) Inherently greater measurement depth for a given penetration. A situation can be imagined in which insufficient penetration precludes a reliable gradient measurement at umbilicus depths due to annual variations which are quickly masked by penetrator induced transients, but for which annual variations at the penetrator depth are negligible. In such a case, only the radial extension design could provide a reliable gradient measurement.

In summary, it is our feeling that the narrow time constraint of the radial extension design is the overriding negative factor in the choice of alternate heat flow measurement techniques. The lunar experience clearly demonstrated the value of a multisensor network which could measure transient and periodic temperature variations as well as the steady state gradient. Unless new information is obtained demonstrating the likelihood of large penetration depths (> 5 m) over much of the martian surface, no design concept which has no chance of measuring seasonal variations can be considered favorable.

The ideal experiment, of course, would include both umbilicus and radially deployed temperature sensors. We would therefore still argue for a serious engineering study of the design feasibilities and limitations of both concepts.

Acknowledgements

This work was supported by NASA Purchase Order Number A-35054-B (DC).

Figure Captions

Figure 1 Diurnal mean temperature versus depth for two models of Mars regolith thermal conductivity temperature dependence. Heat flow, Q = 0, is assumed.

Figure 2 Annual mean temperature versus depth for the two models of Mars conductivity used in Figure 1. The dashed line illustrates a feasible gradient that could be produced by the interior heat loss.

Figure 3 Diurnal variations expected in a 9 cm diameter open hole on Mars compared with fluctuations at comparable regolith depths.

Figure 4-8 Inverse time equilibration curves for sensors deployed radially outward from the penetrator along a steel extension arm. Each figure is distinguished by the radial extension arm length (L_p) and radius (R). Numbers on each curve identify the radial distance (in cm) along the extension arm from the penetrator body. In all cases, a preimpact regolith temperature of 100°K was assumed with the radial probe initially at 200°K and the penetrator body maintained at 200°K. Each model was run for the three feasible values of Mars regolith conductivity shown in the figures.

Figures 9,10 Equilibration curves for the same models as shown in Figures 6 and 7 with the exception that a uniform radial gradient of 2.5°K/cm exists initially along the radial extension arm. Numbers in parentheses identify the initial temperature at the hypothetical sensor location.

Figures 11, 12 Equilibration curves for the same models as shown in Figures 6 and 7 with the exception that a probe conductivity ten times less than stainless steel is assumed.

Figure 13 Mars regolith temperature profiles at two different annual phases for two homogenous models of feasible regolith diffusivities. A simple harmonic variation has been assumed at the surface of 30°K amplitude.

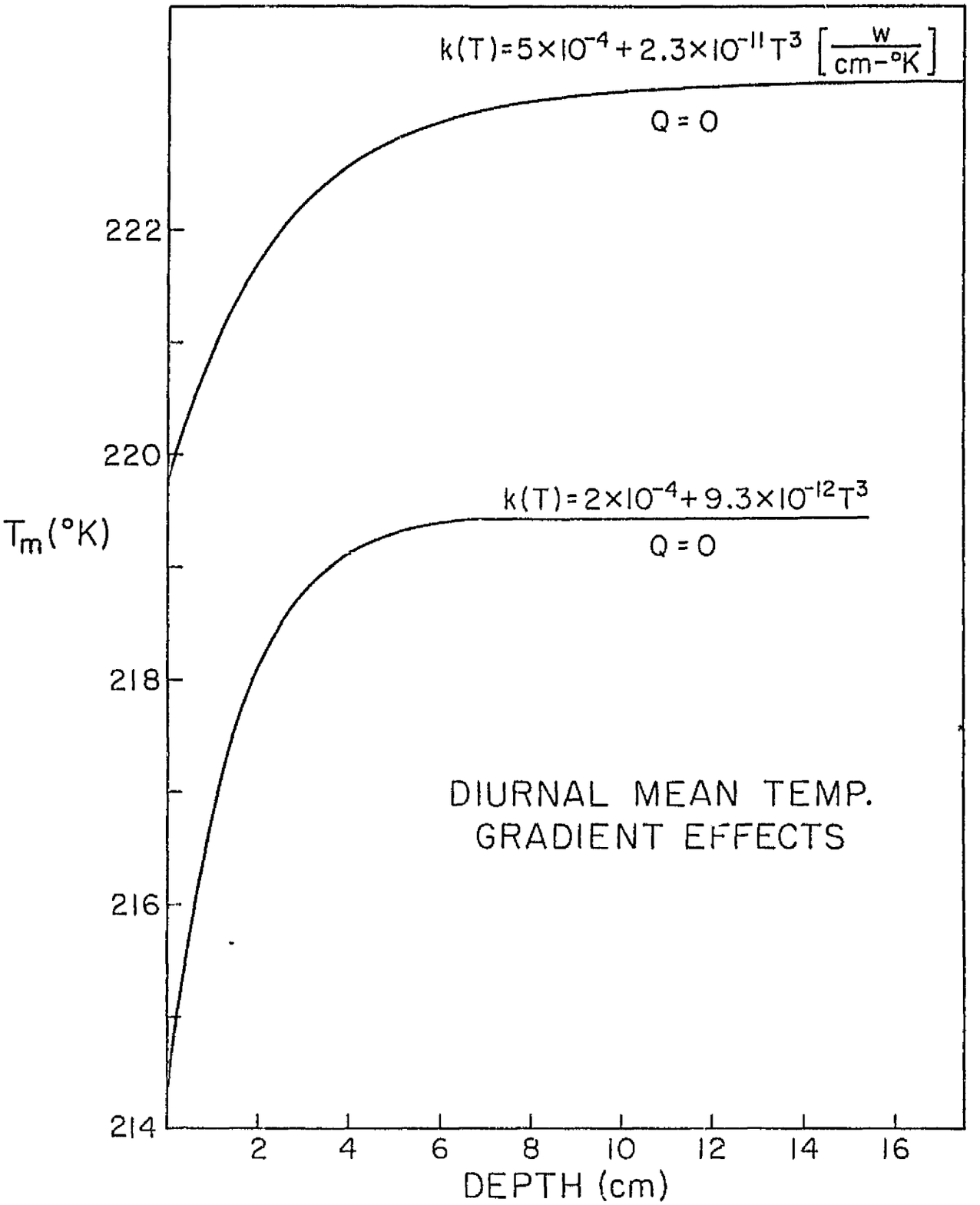
$k(T)=5\times10^{-4}+2.3\times10^{-11}T^3\ \left[\frac{W}{cm-°K}\right]$
Q = 0
$k(T)=2\times10^{-4}+9.3\times10^{-12}T^3$
Q = 0
DIURNAL MEAN TEMP.
GRADIENT EFFECTS
T_m(°K)
222
220
218
216
214
2
4
6
8
10
12
14
16
DEPTH (cm)

Figure 1

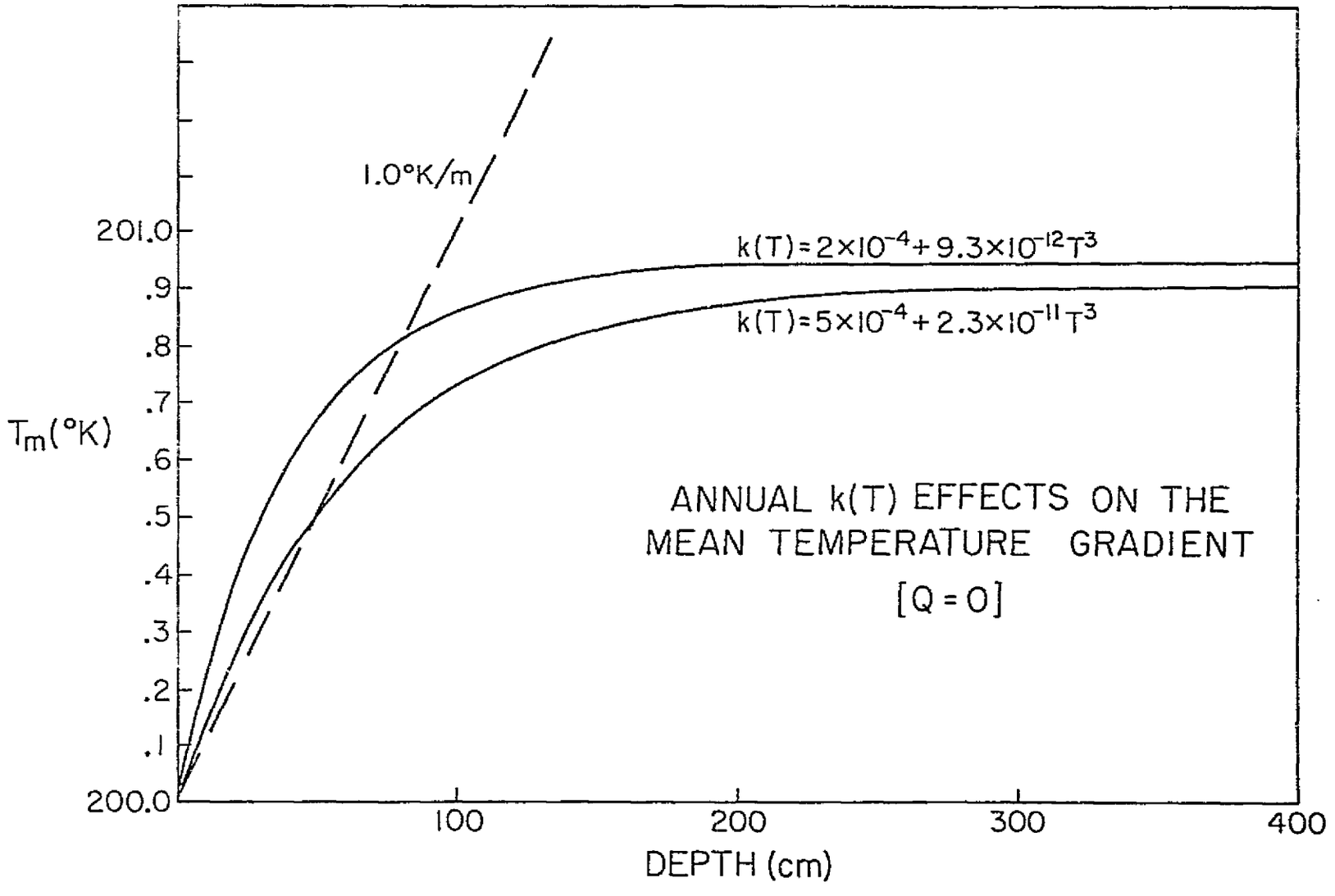
1.0°K/m
k(T)=2×10⁻⁴+9.3×10⁻¹²T³
k(T)=5×10⁻⁴+2.3×10⁻¹¹T³
ANNUAL k(T) EFFECTS ON THE
MEAN TEMPERATURE GRADIENT
[Q = 0]
Tm(°K)
201.0
.9
.8
.7
.6
.5
.4
.3
.2
.1
200.0
100
200
300
400
DEPTH (cm)

Figure 2

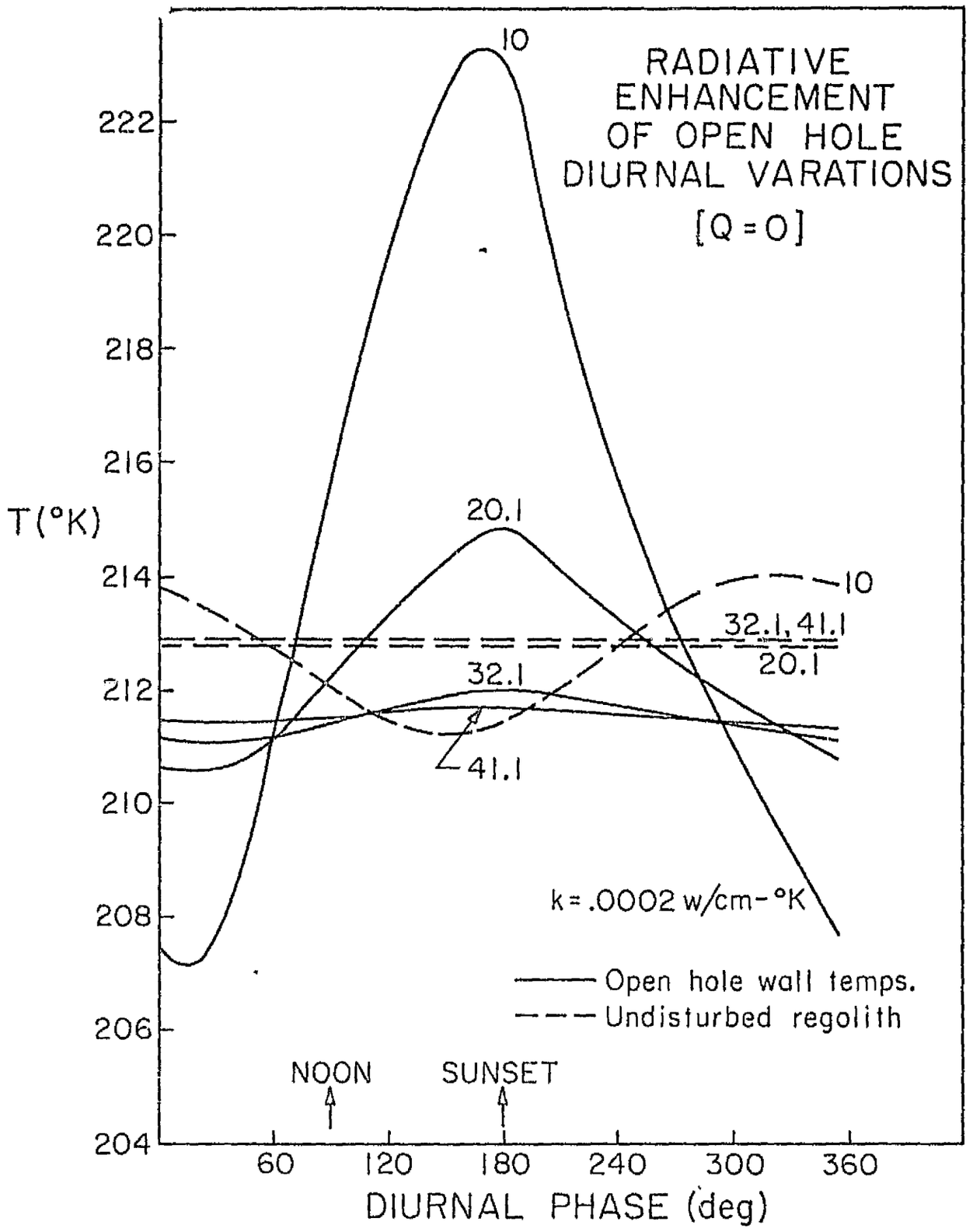
RADIATIVE
ENHANCEMENT
OF OPEN HOLE
DIURNAL VARATIONS
[Q = 0]
10
20.1
32.1
41.1
10
32.1, 41.1
20.1
41.1
k = .0002 w/cm-°K
Open hole wall temps.
Undisturbed regolith
NOON
SUNSET
T(°K)
222
220
218
216
214
212
210
208
206
204
60
120
180
240
300
360
DIURNAL PHASE (deg)

Figure 3

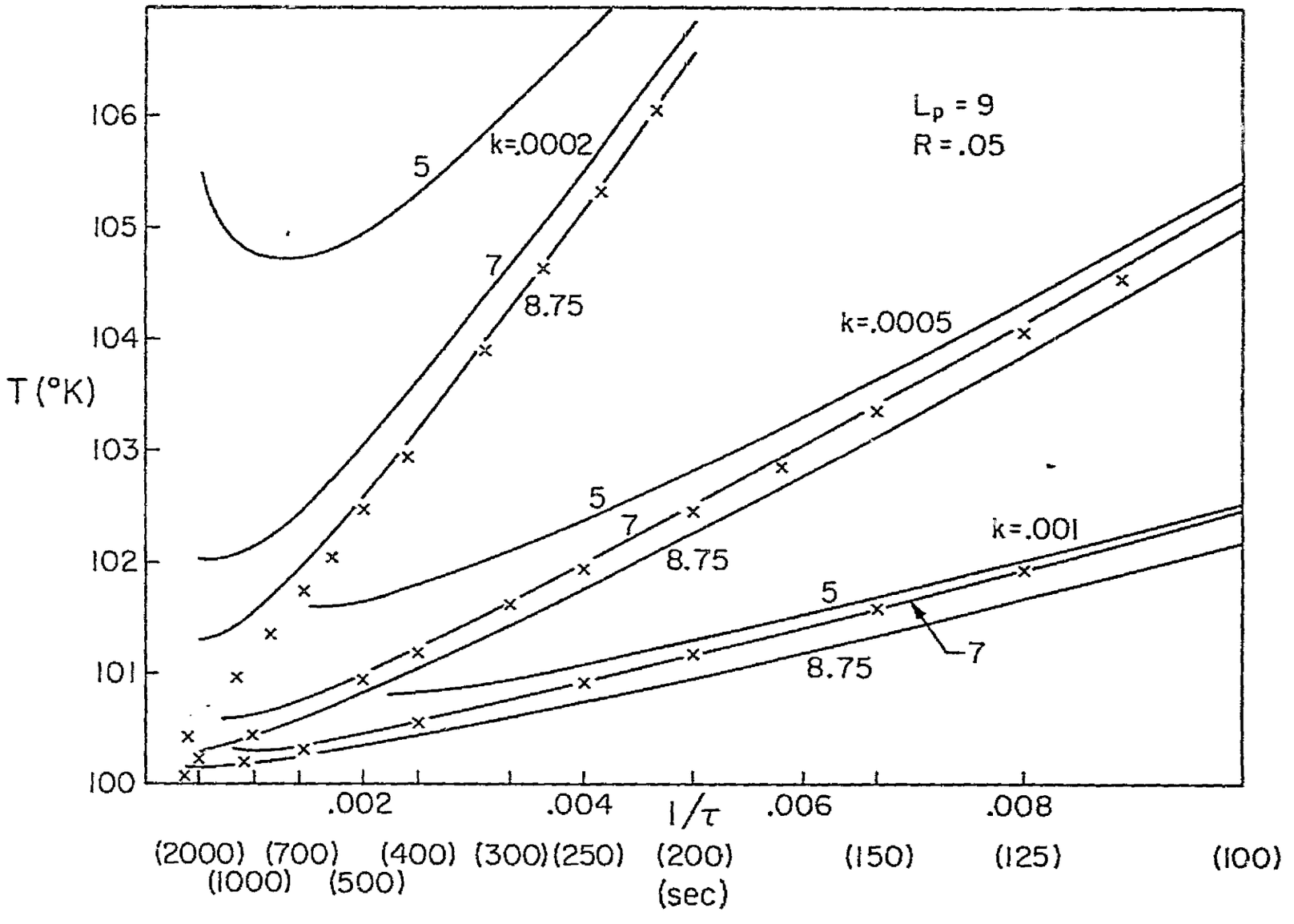
$L_p = 9$
$R = .05$
k=.0002
k=.0005
k=.001
5
7
8.75
T (°K)
106
105
104
103
102
101
100
.002
.004
.006
.008
$1/\tau$
(2000) (1000) (700) (500) (400) (300) (250) (200) (150) (125) (100)
(sec)

Figure 4

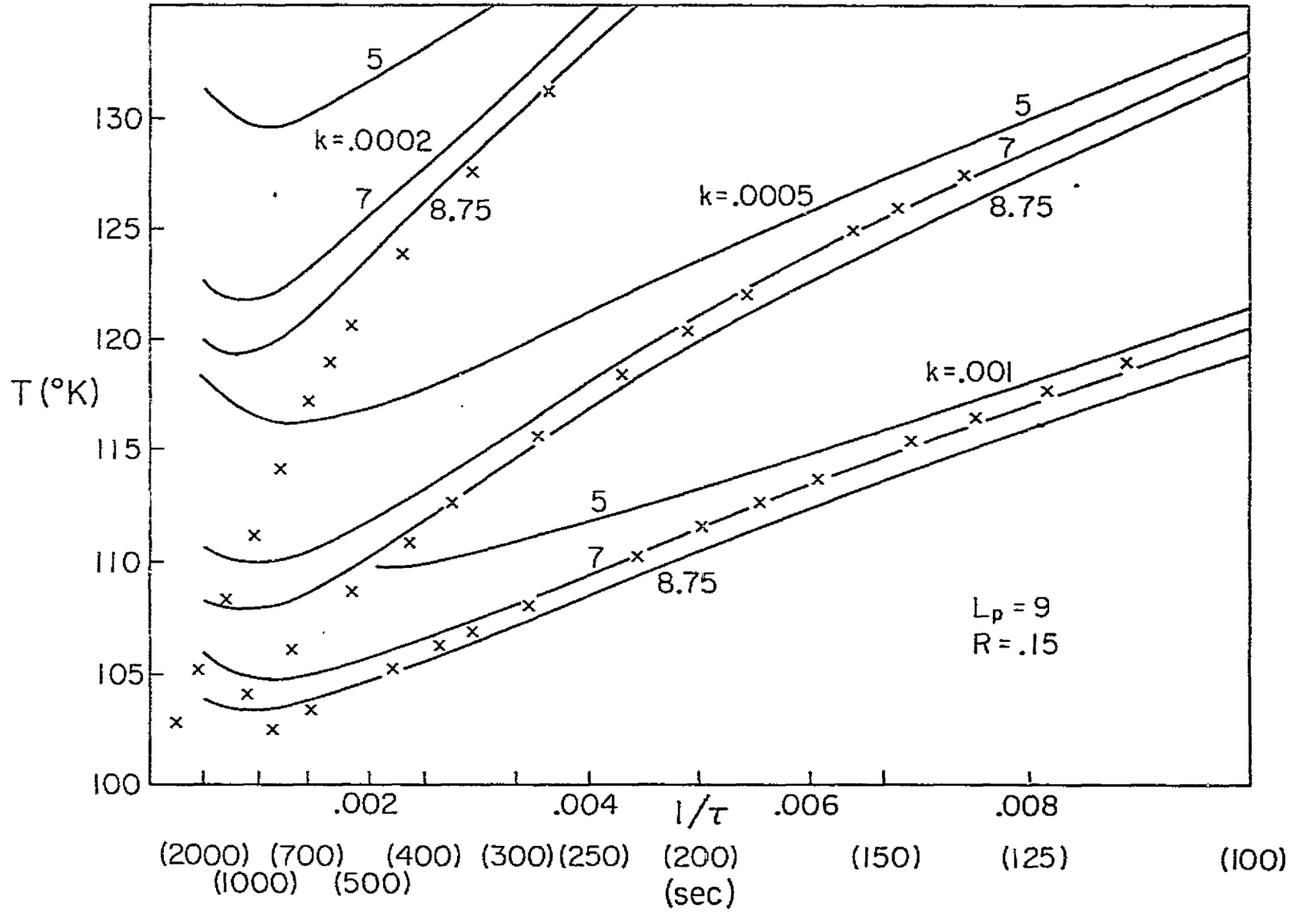

Figure 5

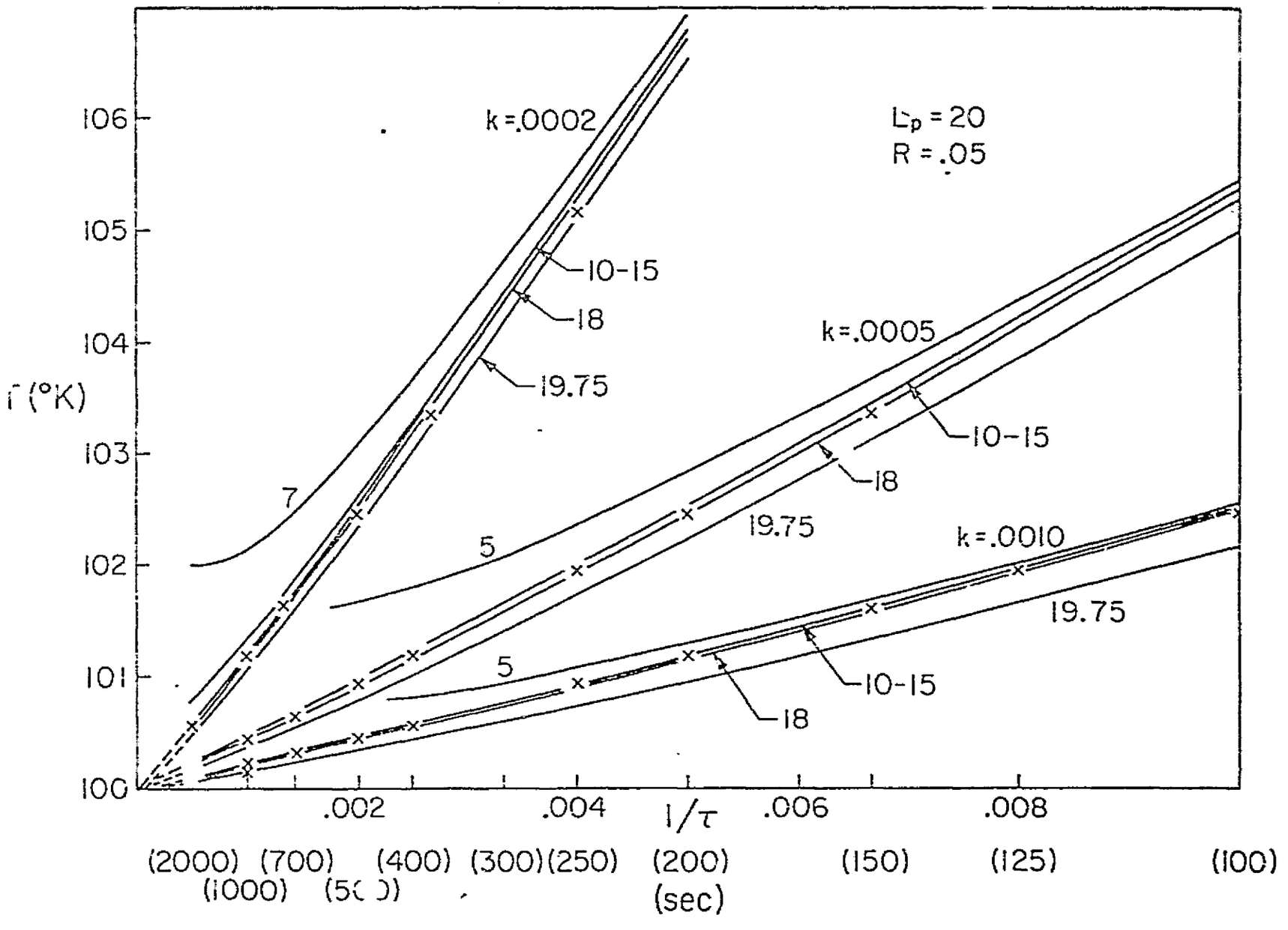
k=.0002
$L_p = 20$
R = .05
10-15
18
19.75
k=.0005
10-15
18
19.75
k=.0010
19.75
10-15
18
7
5
5
106
105
104
103
102
101
100
T (°K)
.002
.004
.006
.008
1/τ
(2000) (700) (400) (300) (250) (200) (150) (125) (100)
(1000) (500)
(sec)

Figure 6

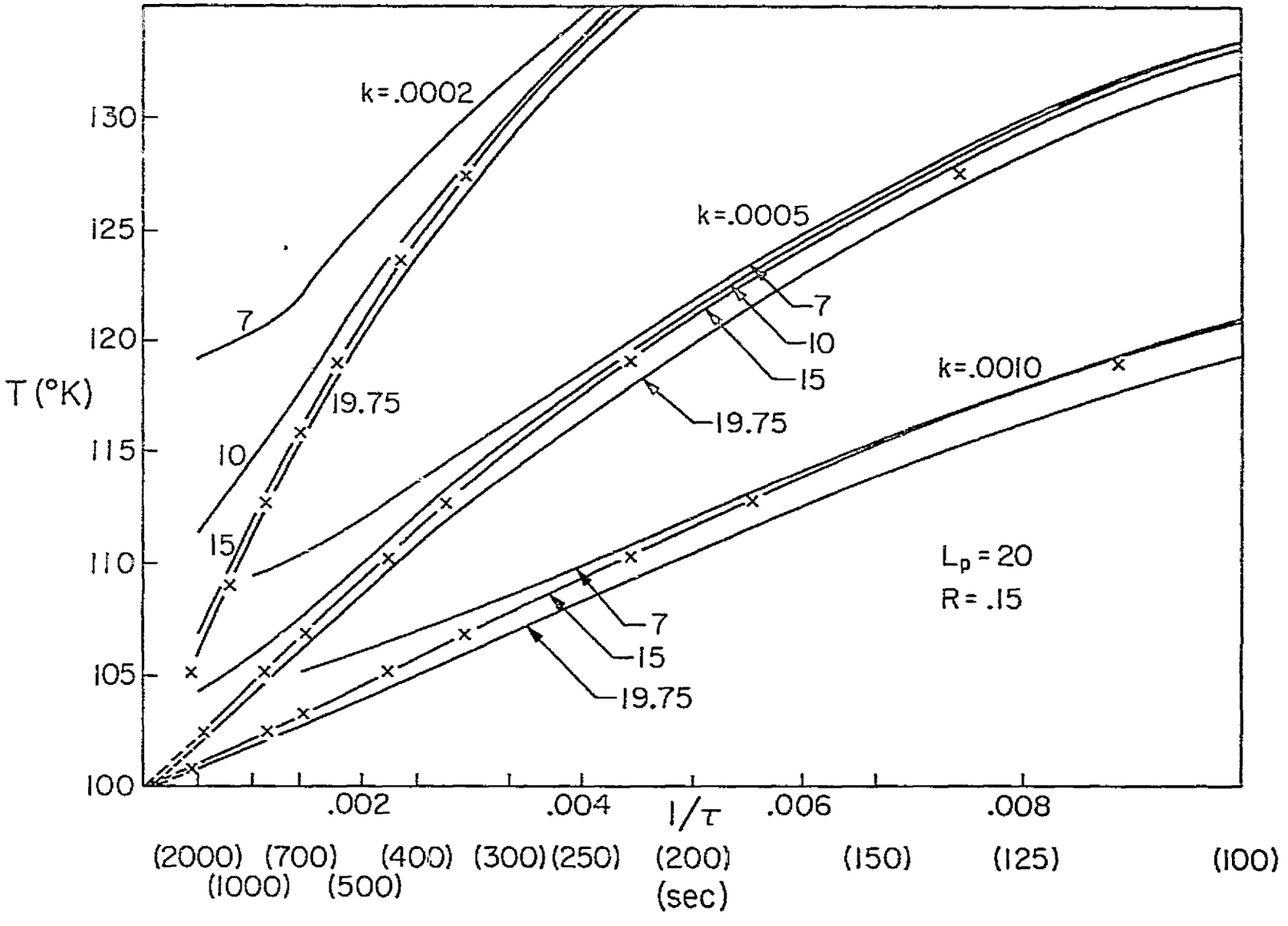
k=.0002
k=.0005
k=.0010
7
10
15
19.75
$L_p = 20$
R = .15
T (°K)
130
125
120
115
110
105
100
.002
.004
.006
.008
1/τ
(2000)
(1000)
(700)
(500)
(400)
(300)
(250)
(200)
(150)
(125)
(100)
(sec)

Figure 7

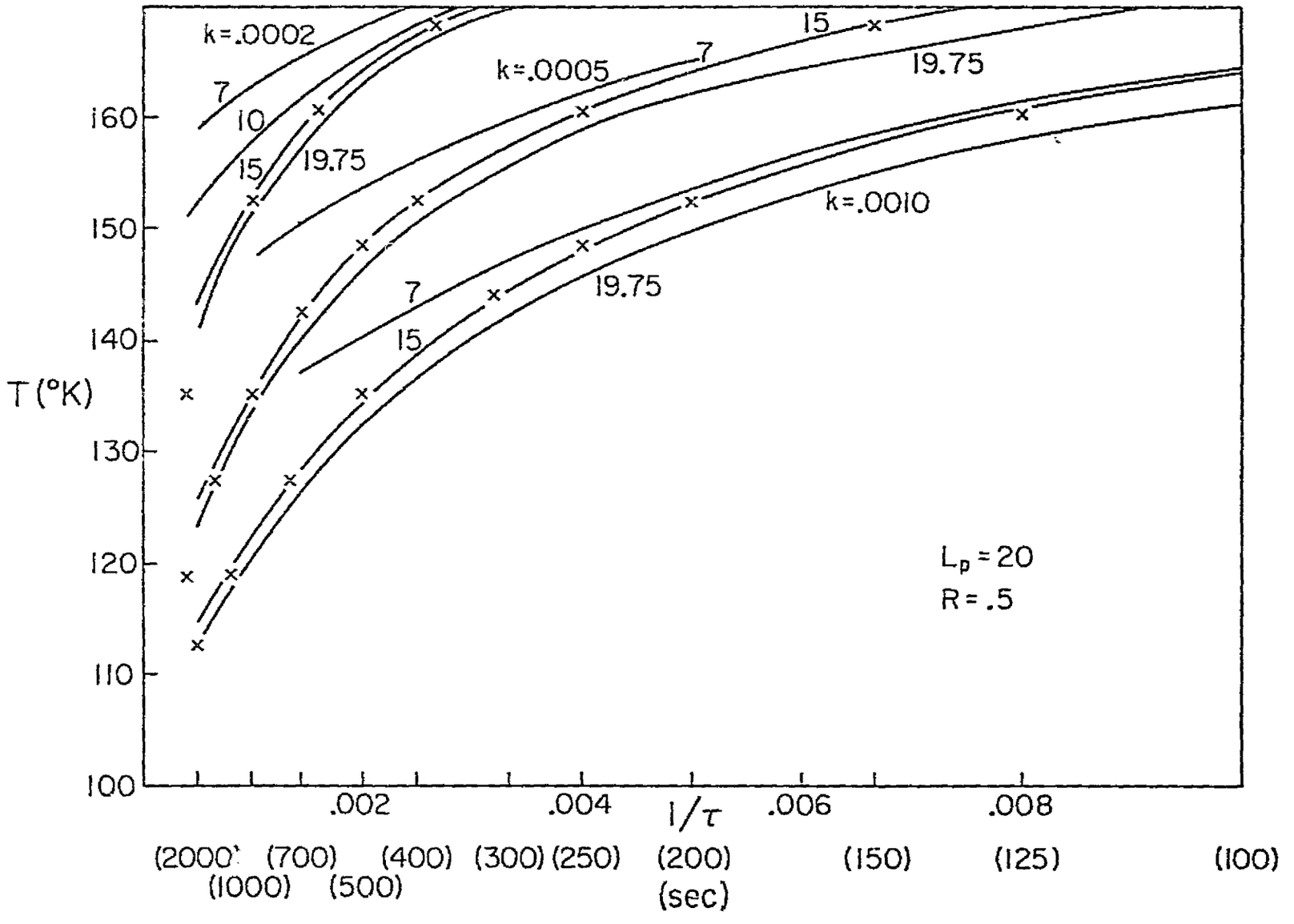
k=.0002
7
10
15
19.75
k=.0005
7
15
19.75
k=.0010
7
15
19.75
160
150
140
130
120
110
100
T (°K)
$L_p = 20$
R = .5
.002
.004
.006
.008
1/τ
(2000) (700) (400) (300) (250) (200) (150) (125) (100)
(1000) (500)
(sec)

Figure 8

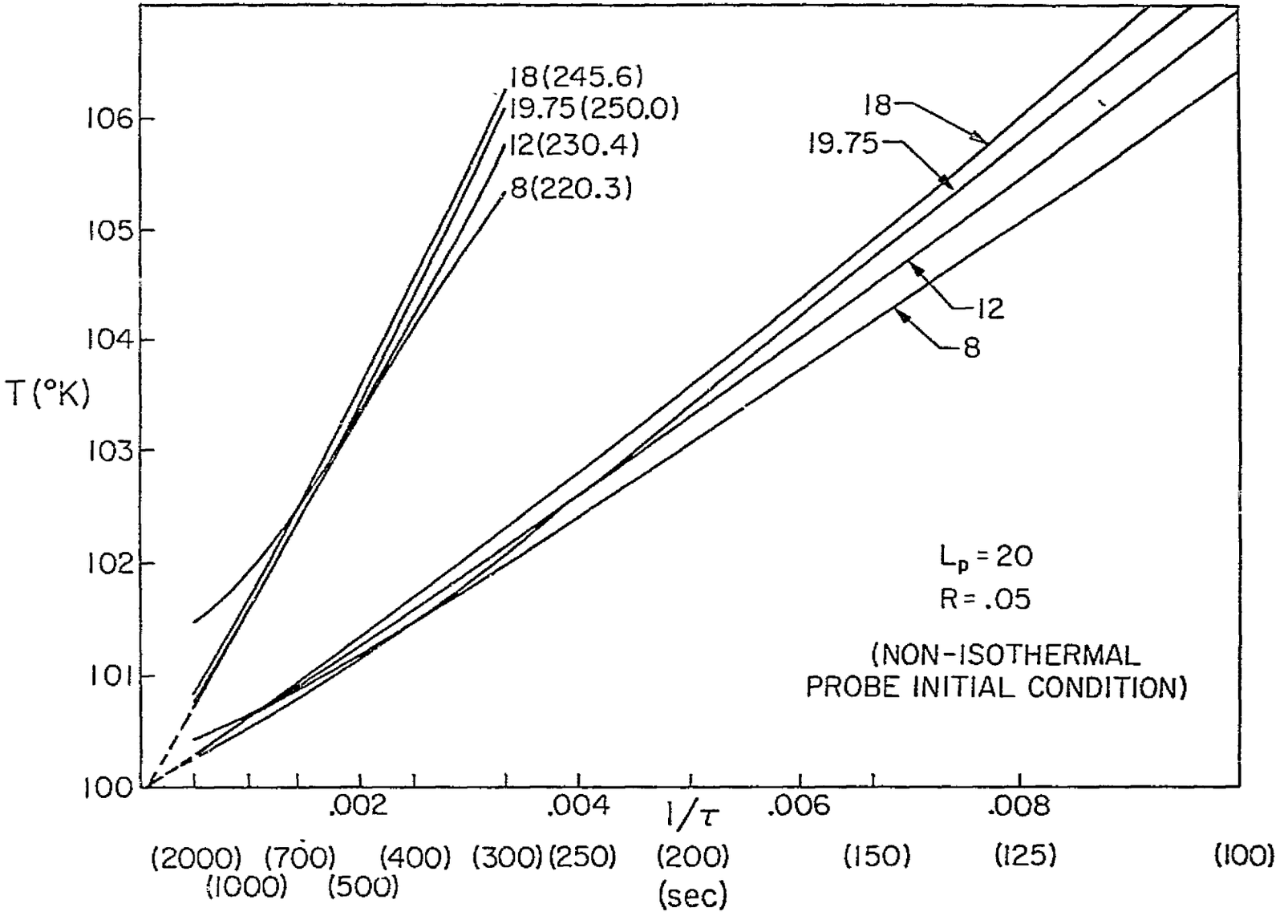
18(245.6)
19.75(250.0)
12(230.4)
8(220.3)
18
19.75
12
8
106
105
104
103
102
101
100
T(°K)
$L_p = 20$
R = .05
(NON-ISOTHERMAL
PROBE INITIAL CONDITION)
.002
.004
.006
.008
1/τ
(2000) (1000) (700) (500) (400) (300) (250) (200) (150) (125) (100)
(sec)

Figure 4

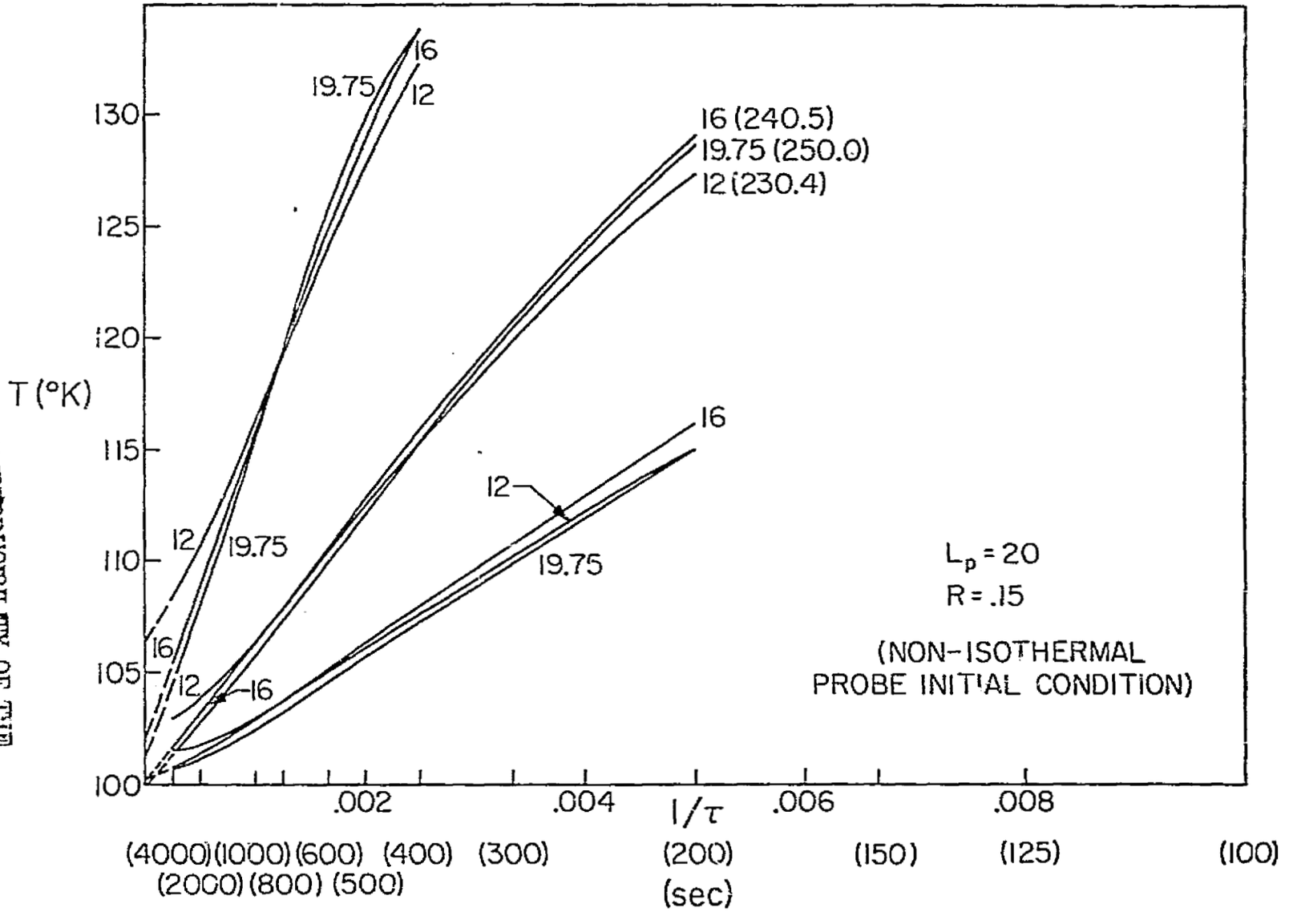

Figure 10

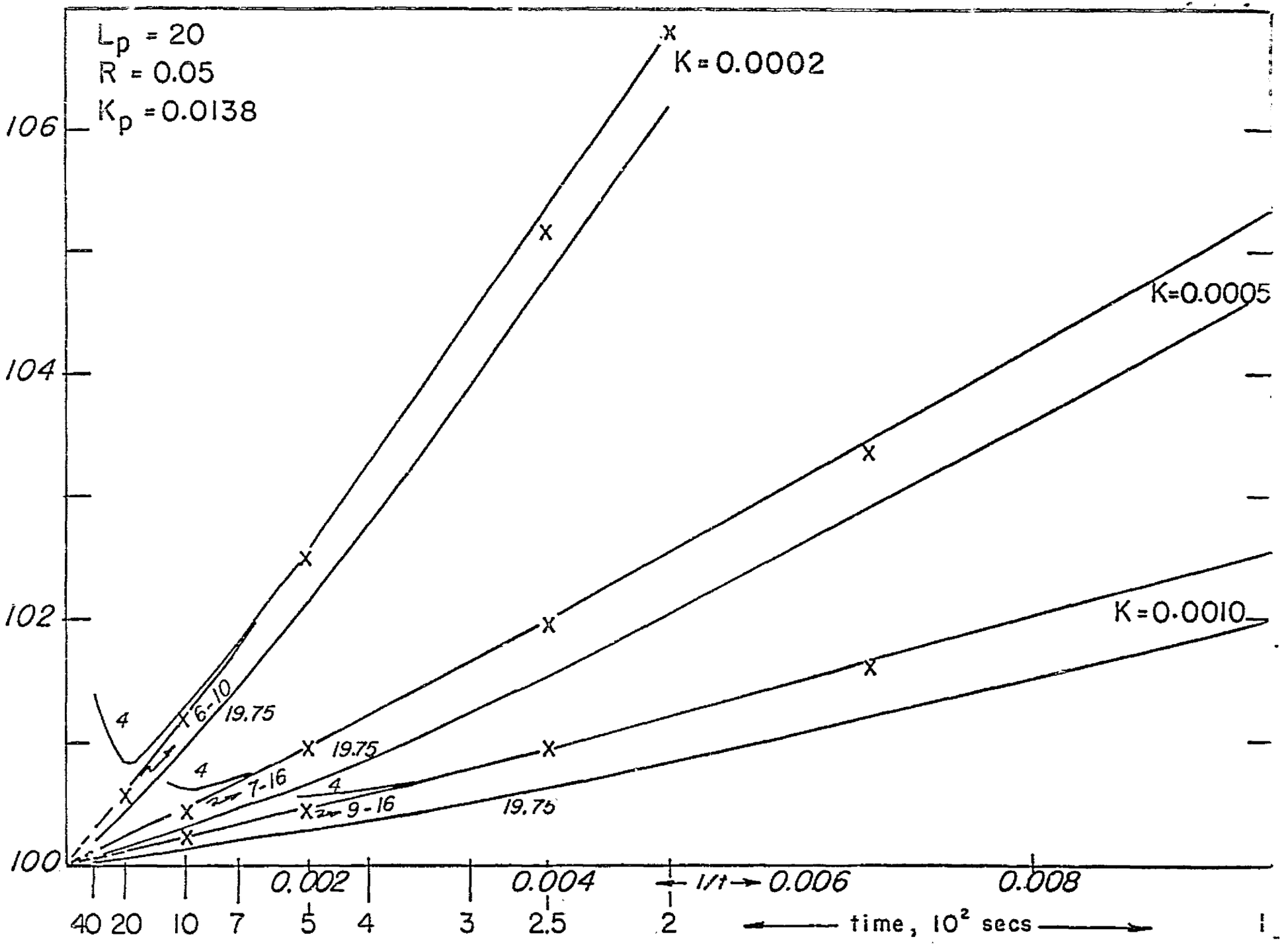
L_p = 20
R = 0.05
K_p = 0.0138
K = 0.0002
K=0.0005
K=0.0010
106
104
102
100
4
6-10
19.75
4
19.75
4
7-16
4
9-16
19.75
0.002
0.004
1/t → 0.006
0.008
40 20 10 7 5 4 3 2.5 2 1
time, 10^2 secs

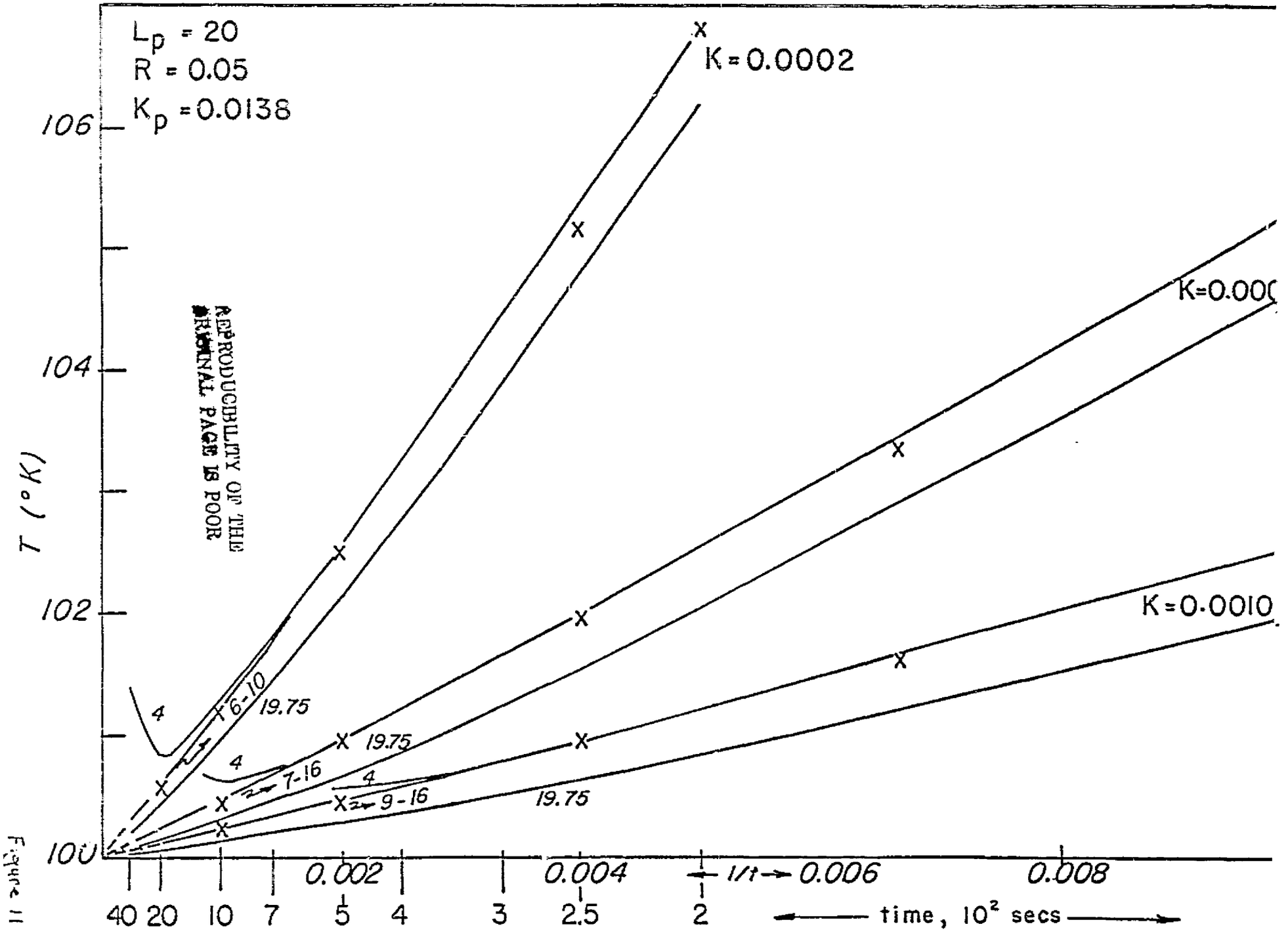

Figure 11

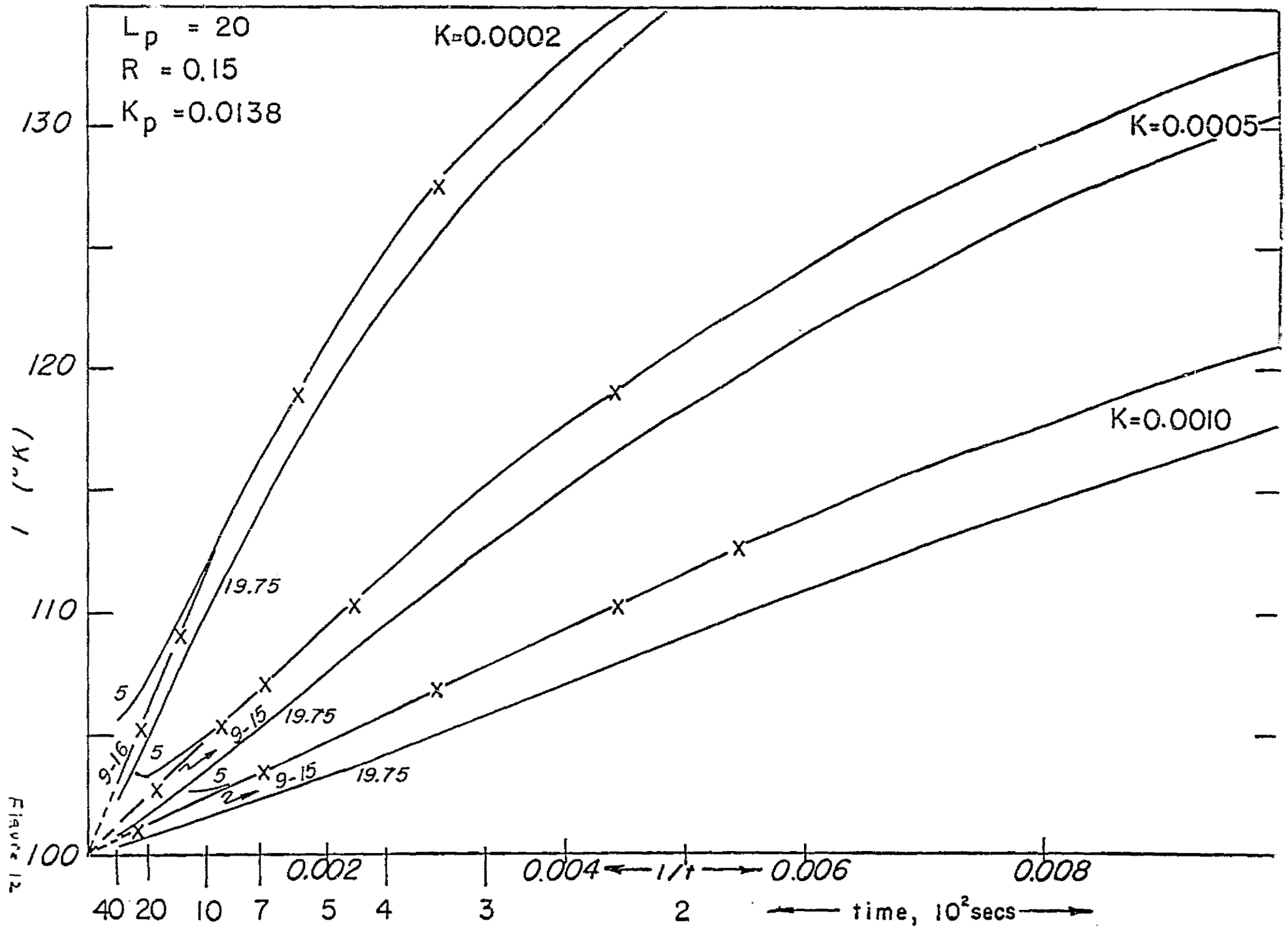
L_p = 20
R = 0.15
K_p = 0.0138
K=0.0002
K=0.0005
K=0.0010
130
120
110
100
T (°K)
19.75
5
9-16
5
9-15
19.75
5
2
9-15
19.75
0.002
0.004
1/t
0.006
0.008
40 20 10 7 5 4 3 2
time, 10^2secs

Figure 12

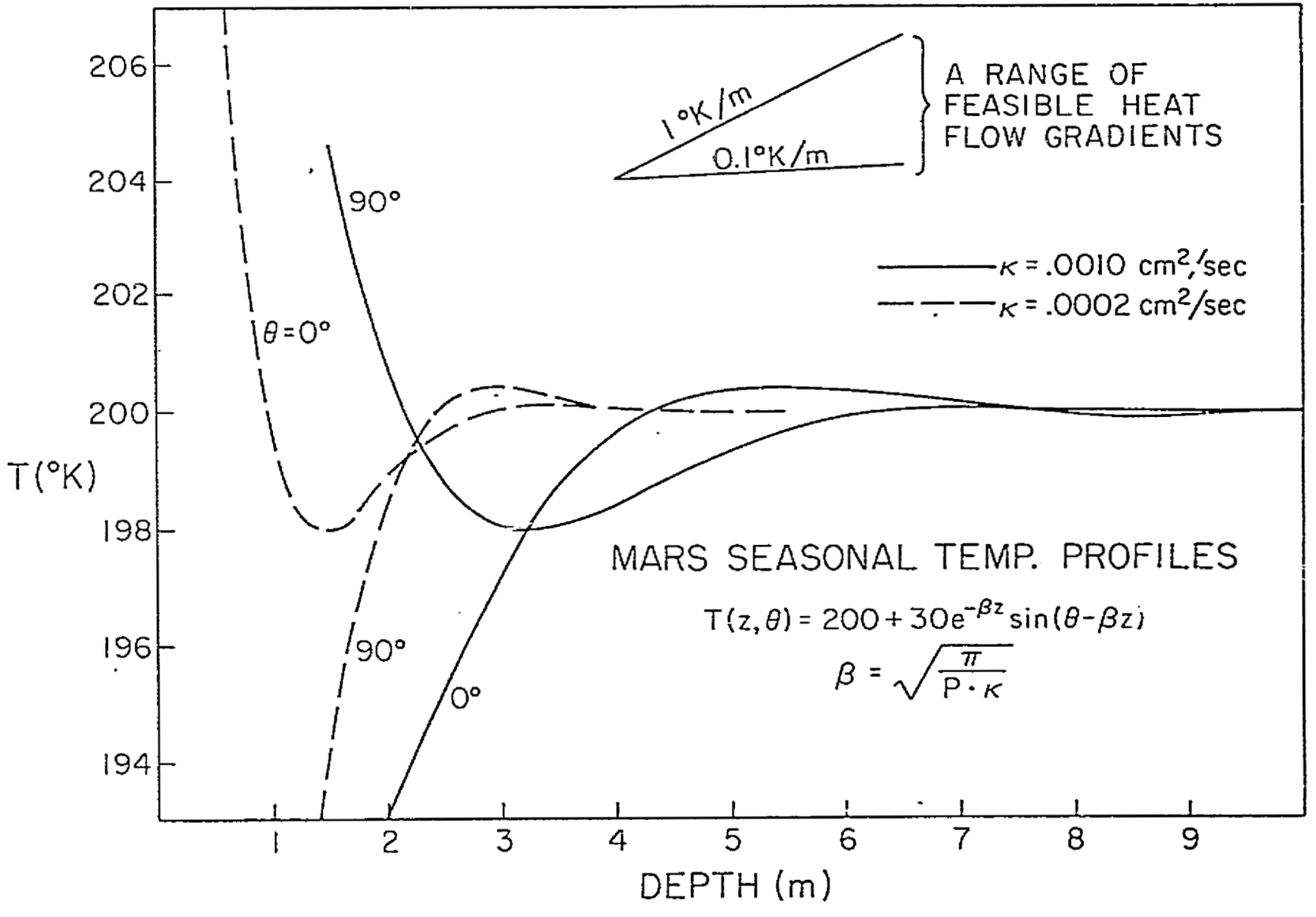
206
204
202
200
198
196
194
T(°K)
1
2
3
4
5
6
7
8
9
DEPTH (m)
1°K/m
0.1°K/m
A RANGE OF FEASIBLE HEAT FLOW GRADIENTS
κ = .0010 cm²/sec
κ = .0002 cm²/sec
θ=0°
90°
90°
0°
MARS SEASONAL TEMP. PROFILES
$T(z,\theta) = 200 + 30e^{-\beta z}\sin(\theta-\beta z)$
$\beta = \sqrt{\frac{\pi}{P\cdot\kappa}}$

Figure 13